IV. OPTICAL AND INFRARED SPECTROSCOPY*

Academic and Research Staff

Professor C. H. Perry

Graduate Students

Jeanne H. Fertel	J. F. Parrish	N. Tornberg
D. Muehlner	J. Reintjes	E. F. Young

A. TRANSMISSION SPECTRA OF (ABF_3) TYPE FLUORIDE PEROVSKITES

1. Introduction

Second-order dipole moments resulting from charge deformation during lattice vibrations are adequate to explain the coupling mechanism for multiphonon processes seen in absorption spectra in the infrared.[1] It is also reported that anharmonic terms in the potential energy function contribute to multiphonon processes.[2] Birman[3] performed a full analysis of the space group for diamond and zinc blende crystal structures to determine general selection rules for electronic transitions, vibrational excitations, and mixtures of both. He applied his results to experimental infrared data of multiphonon combination bands for these structures[4] and was able to assign all observed bands to phonon combinations in agreement with earlier assignments.[5]

The full-space group analysis of the cubic perovskite crystal structure for the determination of selection rules for multiphonon processes has not yet been accomplished; however, the observed multiphonon processes seen in the infrared transmission spectra of the cubic perovskites can be assigned to combinations of phonons at critical points on the lattice dispersion curves of the phonon branches by using the general selection rule of Lax and Burstein,[1] which states that if a crystal has a center of symmetry, multiphonon processes can occur only between phonons coming from different branches in the Brillouin zone.

The transmission spectra of thin single crystals (~70μ) of $KMgF_3$, $KMnF_3$, $KCoF_3$, $KNiF_3$, $KZnF_3$, $RbMnF_3$ and $K(50\%\,Mg + 50\%\,Ni)F_3$ have been viewed from 4000 cm^{-1} t0 20 cm^{-1} at 300°K and 85°K with the use of unpolarized radiation. The absorption bands found in this transmission study and side bands found in a reflectance spectra study of the same materials[6] were assigned to multiphonon processes occurring at the edge of the Brillouin zone. A fitting scheme was proposed and the frequencies of the nine phonon branches at the edge of the zone were determined for this list of fluoride perovskites. Ferguson, Guggenheim, and Wood[7] have reported vibrational intervals observed in the electronic absorption spectra study of the Ni^{++} ion in $KNiF_3$. These

*This work was supported by the Joint Services Electronics Programs (U.S. Army, U.S. Navy, and U.S. Air Force) under Contract DA 36-039-AMC-03200(E).

vibrational intervals have been successfully assigned to combinations of electronic and vibrational transitions not in agreement with the assignments of Ferguson, Guggenheim, and Wood.

2. Discussion

Multiphonon processes appear as continuous absorption of photons and are classified as summation processes if two or more phonons are created, or difference processes if a phonon is annihilated as well as some being created. As a crystal is cooled, summation bands become more intense and difference bands become less intense and disappear when the temperature is sufficiently low.[6] Energy and momentum must be conserved for the initial and final states of the process.

Table IV-1. Frequencies of absorption bands from transmission data on thin samples.

	$KMgF_3$	$KMnF_3$	$KCoF_3$	$KNiF_3$	$KZnF_3$	$RbMnF_3$	$K(50\%\,Mg + 50\%\,Ni)F_3$
a.	403	775	350	324	330	333	407
b.	430		810	354	351	600	710
c.	615			363	362	745	875
d.	632			390	640		
e.	667			585	790		
f.	735			630			
g.	762			667			
h.	794			835			
i.	803			*1210			
j.	827						
k.	857						
l.	911						
m.	943						

Temperature 85°K.
All frequencies in cm^{-1}.
*Seen with thick sample only.

The experimental procedure and the plotted transmission spectra of thin single crystals (~70μ thick) of the fluoride perovskites are published elsewhere.[6] The spectra exhibited the three normal vibrations of the allowed infrared active modes as large absorptions with zero transmission at the positions of the peak frequencies in the reflectance spectra. Table IV-1 lists the absorption bands in the infrared transmission spectra of thin single crystals at 85°K and the largest number of absorptions were found

in $KMgF_3$ and $KNiF_3$. The mixed crystal of K(50% Mg + 50% Ni)F_3, on the other hand, had only 3 observable absorptions as compared with the 21 seen in the pure crystals of $KMgF_3$ and $KNiF_3$. The mixing of the B-ion in the cubic ABF_3 perovskite obscures the infrared absorption bands.

The absorption bands found in the transmission study of thin single crystals were temperature-dependent. The absorptions sharpened and shifted to higher frequencies upon cooling to 85°K and were relatively broad, indicating combinations of lattice vibrations. It did not seem reasonable to assign any of the noted absorptions to pure electronic transitions, as these would be normally quite sharp. The positions of the absorption peaks at 300°K could not be accurately located because of the broad shallow nature of the bands.

The transmission spectrum of each crystal studied at frequencies greater than 1200 cm^{-1} showed no noticeable absorptions, the spectra were flat at approximately 90 per cent transmittance, and the transmission at 300°K and 85°K coincided.

The cubic perovskite crystal structure has three triply degenerate infrared active optical modes, one triply degenerate optically inactive mode, and one triply degenerate acoustical mode.[8] Considering the possible polarizations and degeneracies, the cubic perovskite structure has 9 phonon branches in the Brillouin zone. They are described as follows.

2-TO_1 – transverse optical phonon (lowest frequency) i. r. active
2-TO_2 – transverse optical phonon (middle frequency) i. r. active
2-TO_3 – transverse optical phonon (highest frequency) i. r. active
3-O_4 – optical phonon (frequency unknown) not i. r. or Raman active
1-LO_1 – longitudinal optical phonon (lowest frequency) i. r. active
1-LO_2 – longitudinal optical phonon (middle frequency) i. r. active
1-LO_3 – longitudinal optical phonon (highest frequency) i. r. active
2-TA – transverse acoustical phonon (frequency unknown)
1-LA – longitudinal acoustical phonon (frequency unknown)

Apart from the O_4, TA and LA phonon branches, the frequencies of the other phonon branches at $K \approx 0$ at the center of the Brillouin zone have been determined.[6]

The following restrictions were used to assign multiphonon processes to the observed infrared absorption bands and minor oscillators in the measured reflectance spectra.

1. To a first approximation, all crystals studied had a center of symmetry at 85°K. Therefore, only combinations of phonons from different branches were allowed.[1]

2. Due to the large effective charges of the normal modes of the fluoride perovskites[6] and the qualitative illustration of the effect of ionicity on the vibrational spectrum of a diatomic lattice for large effective charge,[5] the phonon frequencies at the edge of the Brillouin zone were as follows:

a. The frequencies of the transverse optical phonon branches were equal to or

slightly less than their frequencies at $K \approx 0$ at the center of the zone.

b. The frequencies of the longitudinal optical phonon branches were less than their values at $K \approx 0$ at the center of the zone and decreased more than a transverse optical phonon branch when going from the center of the zone to the edge.

c. The frequency of the longitudinal acoustical phonon branch was larger than the transverse acoustical phonon branch.

3. The frequency of the triply degenerate optically inactive phonon branch was unknown. This normal mode was associated, however, with an internal motion of the (BF_3) octahedron and it was assumed to have a frequency similar to the other internal motions of this unit.

There were nine phonon branches at the edge of the Brillouin zone to contribute to multiphonon processes seen as absorption bands in transmission and minor oscillators in reflection. With these restrictions, there were a possible

$$N = \frac{1}{2}\frac{n!}{(n-2)!} = \frac{1}{2}\frac{9!}{(9-2)!} = 36 \qquad (1)$$

two-phonon combinations from different branches to explain multiphonon processes.

The procedure followed to assign the observed multiphonon processes to combinations of phonons from the edge of the Brillouin zone for the cubic fluoride perovskites are listed below.

1. Starting with the frequencies of the transverse phonon branches at $K \approx 0$ at the

Table IV-2. Frequencies of phonon branches at the edge of the Brillouin zone (cm^{-1}) (85°K).

	$KMgF_3$	$KMnF_3$	$KCoF_3$	$KNiF_3$	$KZnF_3$	$RbMnF_3$
TO_1	162	120	132	149	135	109
TO_2	291	191	218	241	195	193
TO_3	471	414	445	450	424	386
O_4	442	325	365	387	338	311
LO_1	181	141	150	150	146	120
LO_2	335	241	255	282	216	224
LO_3	504	450	*	517	452	434
LA	94	70	90	82	70	90
TA	70	64	81	70	66	80

*Not assigned due to a lack of available multiphonon processes.

center of the zone, these frequencies were adjusted until two-phonon combinations of them agreed with as many observed multiphonon processes as possible consistent with the stated restrictions. The fitted frequencies were then assigned to the frequencies of the transverse optical phonon branches at the edge of the zone.

2. The frequencies of the transverse optical phonon branches at the edge of the zone were subtracted from the remaining observed multiphonon processes. Numbers which repeated in this list of subtractions were chosen as possible frequencies of unknown phonon branches at the edge of the zone. This procedure was followed in choosing the remaining six unknown phonon branch frequencies at the edge of the zone and the frequencies were assigned to phonon branches with the help of the list of restrictions placed on the branches.

Tables IV-2 through IV-5 list the frequencies of the phonon branches at the edge of the Brillouin zone and the assignments determined from the best fit to the observed multiphonon absorptions.

Ferguson, Guggenheim, and Wood[7] have observed vibrational intervals in their study of electronic absorption spectra of the Ni^{++} ion in $KNiF_3$ with thin samples at helium temperatures. In a second paper,[9] they assigned the observed vibrational intervals to combinations of $K \approx 0$ optical (transverse) phonon modes with forbidden electronic transitions. The phonons break down the selection rules for forbidden electric dipole transitions. The first four frequencies observed by them in each of the $^3A_{2g} \rightarrow {}^3T^a_{1g}$, $^3A_{2g} \rightarrow {}^1T_{2g}$, and $^3A_{2g} \rightarrow {}^3T^6_{1g}$ transitions were assigned to combinations of the forbidden electronic transition with one of the four transverse optical phonons at $K \approx 0$ from the center of the Brillouin zone. They used the vibrational intervals as a basis for this assignment. A study of their vibrational intervals and the phonon branch frequencies at $K \approx 0$ at the center of the zone and at the edge of the zone[6] have led to the electronic-vibrational assignments given in Table IV-6.

The frequencies of the phonon branches at the edge and at $K \approx 0$ at the center of the Brillouin zone were for 85°K,[6] while Ferguson, Guggenheim, and Wood[7] made their measurements at 4°K. The value of 469 cm^{-1} assigned to the TO_3 branch at $K \approx 0$ at the center of the zone to fit the vibrational intervals was a reasonable assignment for the frequency of the transverse optical phonon branch of $KNiF_3$ at 4°K since this phonon frequency increased as the crystal was cooled from 300°K to 85°K.[6] The frequencies of the remaining phonons were not changed for the assignments of the vibrational intervals at 4°K and the calculated vibrational intervals for the assignments listed in Table IV-6 were very close to those reported.[7]

The first absorption reported by Ferguson, Guggenheim, and Wood[7] was assigned here to the transverse acoustical mode at the edge of the Brillouin zone, the next four, to the transverse optical phonon modes at $K \approx 0$ at the center of the zone in the order of increasing frequency. This gave a frequency of 387 cm^{-1} for the triply degenerate

Table IV-3. Multiphonon assignments to experimental data (85°K).

$KMgF_3$		$KNiF_3$	
Observed frequency	Assignment and calculated frequency	Observed frequency	Assignment and calculated frequency
403	$LO_2 + TA = 405$	324	$TO_2 + LA = 323$
	†$TO_3 - TA = 401$	354	$LO_2 + TA = 352$
430	$LO_2 + LA = 429$	363	$LO_2 + LA = 364$
	†$LO_3 - TA = 434$	390	$TO_1 + TO_2 = 390$
*499	$TO_1 + LO_2 = 497$	*470	$O_4 + LA = 469$
*516	$LO_1 + LO_2 = 516$	*521	$TO_2 + LO_2 = 523$
*541	$TO_3 + TA = 541$	585	$LO_3 + TA = 587$
615	$TO_3 + TA + TA = 611$	630	$TO_2 + O_4 = 628$
632	$TO_1 + TO_3 = 633$	667	$TO_1 + LO_3 = 666$
667	$TO_1 + LO_3 = 666$	835	$TO_3 + O_4 = 837$
735	$TO_2 + O_4 = 733$	1210	$TO_3 + LO_3 + TO_2 = 1208$
762	$TO_2 + TO_3 = 762$		
794	$TO_2 + LO_3 = 795$		
803	$TO_3 + LO_2 = 806$		
827	$LA + O_4 + TO_2 = 827$		
857	$LA + TO_3 + TO_2 = 856$		
911	$TO_3 + O_4 = 913$		
943	$LO_3 + O_4 = 946$		

*Seen in reflection.

†Difference bands.

All frequencies in (cm^{-1}).

Table IV-4. Multiphonon assignments to experimental data (85°K).

$K(50\%\ Mg + 50\%\ Ni)\ F_3$

Observed frequency	Assignment and calculated frequency	Pure crystal
407	$LO_2 + TA = 405$	($KMgF_3$)
*527	$TO_2 + LO_2 = 523$	($KNiF_3$)
	$TO_1 + O_4 = 536$	"
	$LO_1 + O_4 = 537$	"
	$TO_3 + LA = 532$	"
	$TO_3 + TA = 520$	"
	$O_4 + LA = 536$	($KMgF_3$)
710	$TO_2 + TO_3 = 691$	($KNiF_3$)
	$LO_2 + TO_3 = 732$	"
	$TO_2 + O_4 = 733$	($KMgF_3$)
	$LO_1 + LO_3 = 685$	"
875	$TO_1 + TO_3 + LO_2 = 882$	($KNiF_3$)
	$TA + LO_3 + LO_2 = 869$	"
	$LA + LO_3 + LO_2 = 881$	"
	$O_4 + LO_2 + LA = 821$	($KMgF_3$)
	$TO_3 + LO_2 + TA = 876$	"
	$TO_2 + LO_3 + LA = 889$	"
	$LO_1 + LO_1 + LO_3 = 886$	"

*Seen in reflection.

All frequencies in (cm^{-1}).

Table IV-5. Multiphonon assignments to experimental data (85°K).

$KMnF_3$		$KCoF_3$	
Observed frequency	Assignment and calculated frequency	Observed frequency	Assignment and calculated frequency
*261	$TO_1 + LO_1 = 261$	*231	$LO_1 + TA = 231$
	† $O_4 - TA = 261$	*240	$LO_1 + LA = 240$
	$TO_2 + LA = 261$	350	$TO_1 + TO_2 = 350$
*432	$TO_2 + LO_2 = 432$	*473	$TO_2 + LO_2 = 473$
*445	$TO_1 + O_4 = 445$	810	$TO_3 + O_4 = 810$
775	$LO_3 + O_4 = 775$		

$KZnF_3$		$RbMnF_3$	
Observed frequency	Assignment and calculated frequency	Observed frequency	Assignment and calculated frequency
*201	$TA + TO_1 = 201$	*200	$TO_1 + LA = 199$
*205	$LA + TO_1 = 205$		$LO_1 + TA = 200$
330	$TO_2 + TO_1 = 330$	333	$TO_1 + LO_2 = 333$
351	$LO_2 + TO_1 = 351$	*420	$TO_2 + LO_2 = 417$
362	$LO_1 + LO_2 = 362$		$TO_1 + O_4 = 420$
*473	$TO_1 + O_4 = 473$	*431	$LO_1 + O_4 = 431$
640	$TO_3 + LO_2 = 640$	600	$TO_3 + LO_2 = 610$
790	$LO_3 + O_4 = 790$	745	$LO_3 + O_4 = 745$

*Seen in reflection.

†Difference band.

All frequencies in (cm^{-1}).

Table IV-6. Assignment of electronic-vibrational spectrum of $KNiF_3$ reported by Ferguson, Guggenheim, and Wood.[7]

Measured vibrational interval (°K)	Assignment	Calculated vibrational interval
	Pure electronic (E)	
	$E + TA(e) = E + 70$	
81	$E + TO_1(c) = E + 150$	80
177	$E + TO_2(c) = E + 248$	178
317	$E + O_4(c) = E + 387$	317
399	$E + TO_3(c) = E + 469$	399
487	$E + TO_2(c) + LO_2(c) = E + 556$	486
546	$E + LO_2(c) + LO_2(c) = E + 616$	546
625	$E + LO_2(c) + O_4(c) = E + 695$	625
709	$E + LO_3(c) + TO_2(c) = E + 782$	712
832	$E + LO_3(e) + O_4(e) = E + 904$	834

(c) Phonon at $K \approx 0$ from center of Brillouin zone.

(e) Phonon from edge of Brillouin zone.

All frequencies in (cm^{-1}).

optically inactive mode, agreeing with the assignment made earlier (see Table IV-2). The remaining vibrational intervals were assigned to multiphonon processes.

E. F. Young, C. H. Perry

References

1. M. Lax and E. Burstein, Phys. Rev. 97, 39 (1955).
2. B. Szigeti, Proc. Roy. Soc. (London) A252, 217 (1959).
3. J. L. Birman, Phys. Rev. 127, 1093 (1962).
4. J. L. Birman, Phys. Rev. 131, 1489 (1963).
5. R. W. Keyes, J. Chem. Phys. 37, 72 (1962).
6. E. F. Young, Ph. D. Thesis, M. I. T., August 22, 1966.
7. J. Ferguson, H. J. Guggenheim, and D. L. Wood, J. Chem. Phys. 40, 822 (1964).
8. G. R. Hunt, C. H. Perry, and J. Ferguson, Phys. Rev. 134, A688 (1964).
9. J. Ferguson and H. J. Guggenheim, J. Chem. Phys. 44, 1095 (1966).

B. FERROELECTRIC "SOFT" MODE IN $KTaO_3$

Far infrared reflectance measurements have been made on single crystals $KTaO_3$ from 40-1000 microns (250-10 cm^{-1}) over the temperature range 12-463°K. The reflectance data were analyzed using a Kramers-Kronig method to obtain total conductivity, σ, from the imaginary part of the dielectric constant. The conductivity exhibits a very strong temperature dependent low-frequency peak which moves from 106 cm^{-1} at 463°K, to 25 cm^{-1} at 12°K and accounts for more than 90 per cent of the static dielectric constant, ϵ_o.

The results indicate a relationship between this low transverse optical mode, ω_{t_1} for $\underline{k} \approx 0$ and the static dielectric constant ϵ_o, such that

$$\omega_{t_1}^2(T) = A/\epsilon_o(T)$$

where $A = 1.9 \times 10^6$ (cm^{-1}).[2] This result can be related directly to the Curie-Weiss law behavior of ferroelectrics and the associated implications have been derived and discussed by several authors.[1-3] Consequently, the experimental verification in the case of $KTaO_3$ helps confirm the theory of ferroelectricity in perovskite type materials which indicate a soft mode lowering its frequency and becoming unstable as the temperature is lowered towards the Curie point. This phenomenon had previously only been observed with any certainty for $SrTiO_3$ using far infrared[4] and neutron techniques.[5]

The infrared reflectance measurements at a 10° angle of incidence were performed on a Michelson spectrophotometer[6] using several beam splitters and a liquid-helium cooled germanium detector. The sample was mounted in a separately evacuable chamber and its temperature was measured with two calibrated thermocouples attached to the crystal. The complete temperature range could be accomplished without disturbing the sample and mount.

The total reflectivity curve from 10-4000 cm^{-1} was measured at 296°K, and also at 126°K but very little temperature dependence of the modes at about 200 cm^{-1}, 550 cm^{-1} and the side band at 760 cm^{-1} was observed. The results at room temperature agreed closely with those of Miller and Spitzer[7] and reference should be made to their work for the complete spectrum. Between 0-10 cm^{-1} the extrapolated curves were in good agreement with the reflectivity values calculated from the static dielectric constant measurements of Rupprecht and Bell[8] and Davis.[9] Beyond 250 cm^{-1}, the reflectance curve measured at room temperature was used with the high temperature and room temperature data, while the 126°K curve was coupled with the measurements at other temperatures in order to evaluate the far infrared complex dielectric constant from the Kramers-Kronig analysis. The marked temperature dependence of the reflectivity curve below 100 cm^{-1} can be clearly seen in Fig. IV-1, together with the weakly

temperature dependent mode at 200 cm^{-1}.

The frequencies of the normal optically active transverse modes were derived from peaks in the conductivity $\sigma(\omega)$, where $\sigma_j = \epsilon_j'' \omega/2$ and ϵ_j'' is the contribution of the j^{th} resonance to the imaginary part of the dielectric constant.[10]

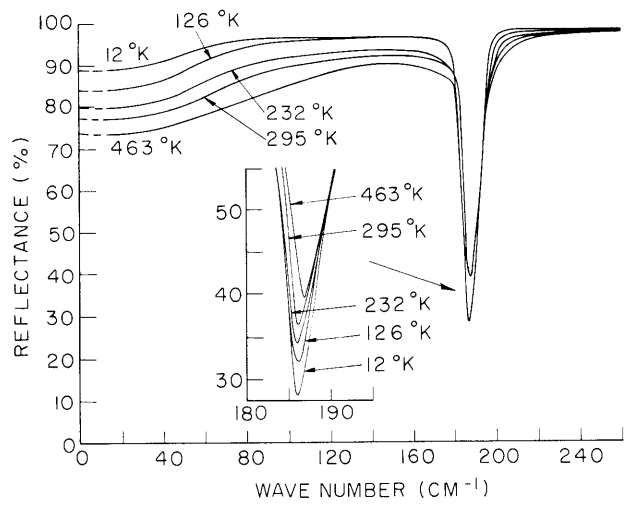

Fig. IV-1. Far infrared reflectivity of $KTaO_3$ as a function of temperature over the frequency range 10-250 cm^{-1}. The error in measurements ≈±2%.

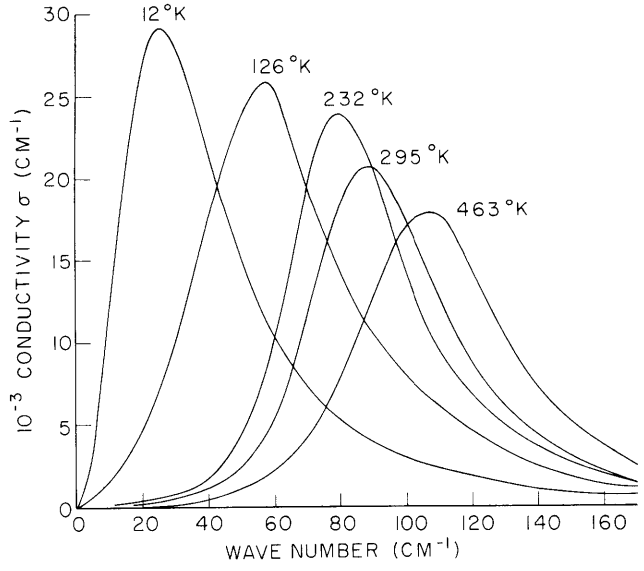

Fig. IV-2. Conductivity calculated from the reflectivity curves shown in Fig. IV-1 for the five different temperatures.

The frequency dependence of the conductivity with temperature below 170 cm^{-1} is shown in Fig. IV-2 and the positions of the "soft" mode are estimated to be accurate to about ±5 cm^{-1}. This estimate was obtained by varying the low frequency input data to the K-K analysis over the limit of the error (±2%) in the reflectance measurements.

The temperature dependence of the transverse optical modes are given in Table IV-7.

The static dielectric constant ϵ_o can be written in terms of the Curie law

$$\epsilon_o \propto \frac{1}{T - T_c},$$

and consequently $\omega_{t_1}^2 \propto T - T_c$. Measurements of ϵ_o for $KTaO_3$ at microwave frequencies by Rupprecht and Bell[8] from 80-303°K have indicated a modified Curie law behavior such that $\epsilon_o = \frac{B}{T - T_c} + C$, where $B = 5.989 \times 10^4$°K, C = 39.32 and the Curie temperature T_c = 2.9°K. This result is shown by the solid curve in Fig. IV-3 together with the temperature dependence of the low frequency mode. The upper four points fall closely on the

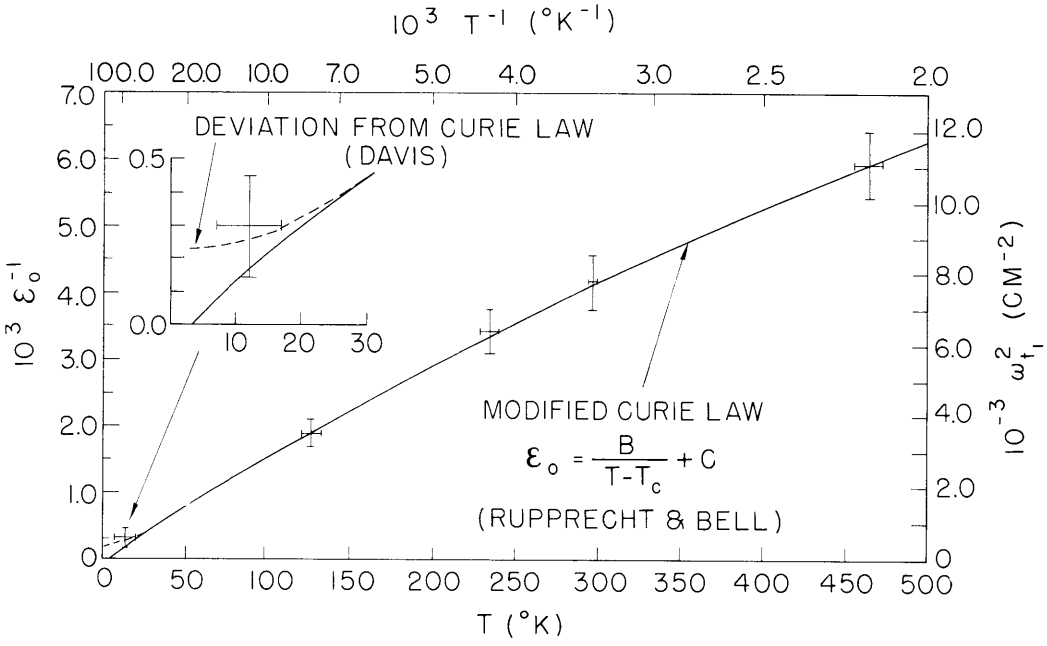

Fig. IV-3. The square of the frequency (in cm^{-1}) of the ferroelectric "soft" mode plotted as a function of temperature. Vertical lines indicate the $\omega_{t_1}^2$ error and horizontal lines show the temperature variation. The solid curve shows the reciprocal of the dielectric constant from the results of Rupprecht and Bell. The extrapolated curves gives a Curie temperature of 2.9°K. The dotted curve shows the low-temperature deviation (below 30°K) from the modified Curie law (R & B) obtained by Davis.

Table IV-7. The transverse optical modes in $KTaO_3$ as a function of temperature.

T°K	ω_{t_1}	ω_{t_2}	ω_{t_3}
12	25	196	–
126	58	198	551
232	79	198	551
295	88*	199*	550*
463	106	199	–

*See Miller and Spitzer[7] for complete spectrum.

modified Curie law described by Rupprecht and Bell but the experimental error in $\omega_{t_1}^2$ barely excludes normal Curie law behavior. Davis[9] has recently measured the dielectric constant below 80°K and has found deviations from the Curie law under 30°K. The one measured frequency in this region (~12°K) also indicates a value corresponding to deviations found by Davis. The extremely low "Curie temperature" makes this crystal ideal for the investigation of the "soft" mode in the paraelectric cubic state. The temperature variation of this vibration is in good agreement with the temperature dependence of the dielectric constant related by the Cochran-Cowley[1,11] theory of ferroeletricity in perovskite crystals.

We would like to thank Professor A. Smakula, Materials Center for Science and Engineering, Massachusetts Institute of Technology, for the sample. All computations were performed on the IBM 7094 computer at the M. I. T. Computation Center.

C. H. Perry, T. F. McNelly

[T. F. McNelly is now in the Physics Department, Cornell University. His work was supported in part by Air Force Cambridge Research Laboratories under contract number AF19-(628)-395.]

References

1. W. Cochran, Advances in Physics, edited by N. F. Mott (Taylor and Francis, Ltd., London, 1960), Vol. 9, p. 387.
2. P. W. Anderson, Fizika Dielectrikov, edited by G. I. Skanavi (Akad. Nauk S.S.S.R. Fizicheskii Inst. im P. N. Lebedeva, Moscow, 1960).
3. T. Nakamura, The Institute for Solid State Physics, Tokyo, Japan, Ser. A, 186, 1 (1966). J. Phys. Soc. Japan, p. 491 (1966).
4. A. S. Barker, Jr. and M. Tinkham, Phys. Rev. 125, 1527 (1962).
5. R. A. Cowley, Phys. Rev. Letters 9, 159 (1962).
6. C. H. Perry, R. Geick, and E. F. Young, Applied Optics 5, 1171 (1966).
7. R. C. Miller and W. G. Spitzer, Phys. Rev. 129, 94 (1963).
8. G. Rupprecht and R. O. Bell, Phys. Rev. 135, A748 (1964).
9. T. G. Davis, S.M. Thesis, Department of Electrical Engineering, M.I.T. (1966).
10. F. Seitz, Modern Theory of Solids (McGraw-Hill Book Co., New York, 1940), Chap. XVII, p. 635.
11. W. Cochran and R. A. Cowley, J. Phys. Chem. Solids 23, 447 (1962).